Available online at www.sciencedirect.com

ScienceDirect

Ceramics International 40 (2014) 1311–1319

CERAMICS INTERNATIONAL

www.elsevier.com/locate/ceramint

Synthesis of nano α-alumina powders using hydrothermal and precipitation routes: a comparative study

Shaghayegh Ghanizadeh*, Xujin Bao, Bala Vaidhyanathan, Jon Binner

Department of Materials, Loughborough University, Loughborough LE11 3TU, UK

Received 9 May 2013; received in revised form 30 June 2013; accepted 1 July 2013
Available online 13 July 2013

Abstract

Two different synthesis methods, viz. precipitation and hydrothermal treatment, were used to synthesise ultra-fine α-alumina powders from aluminium chloride, ammonia solution and TEAH (tetraethyl ammonium hydroxide). XRD, BET surface area analysis, TEM and FEG-SEM were used to characterise the powders produced. The presence of industrial α-alumina powder as seed particles did not affect the transformation to α-alumina phase during the hydrothermal treatment at 220 °C, either in basic or acidic environments. The results obtained from the precipitation route, however, showed that the combined effect of adding α-alumina seeds and surfactants to the precursor solution could lower the transformation temperature of α-alumina from about 1200 °C for unseeded samples to about 800 °C, as well as reducing the level of agglomeration in the alumina powders. The difference in transformation temperature mainly results from the nucleation process caused by the α-alumina seeds, which enhanced the $\theta \rightarrow \alpha$ transformation kinetics. The lower level of agglomeration present in the final powders could be due to a surface modifying role of the surfactants, preventing the particles from coalescing during the synthesis process.

Keywords: Nanoparticle; Al_2O_3; Hydrothermal; Precipitation

1. Introduction

Alumina ceramics have found various technological applications as high-strength materials and in electronics and catalysts because of their distinctive combination of physicochemical properties including hardness, resistance to aggressive media, refractoriness and electrical and thermal insulation [1,2]. In recent years, increasing attention has been focused on the development of alumina powders with particle sizes at the nanoscale for advanced engineering applications such as transparent armours for ballistic performance [3,4].

Reducing the dimensions of a particulate material from microscale to nanoscale leads to considerable changes, both in the physical properties, such as electronic conductivity and optical absorption, and the mechanical properties since a much greater fraction of the atoms are located on the surfaces of the particles [5]. Nano-sized powders have an extremely high surface area, resulting in changes in both surface energy and surface morphology. These parameters then alter the basic properties and the chemical reactivity of the nanomaterials [6]. For instance, some nanocrystalline ceramics have demonstrated superplastic behaviour at elevated temperatures, enabling these ceramics to undergo up to 300% elongation before failure [6]. They have also been used as solid state bonding agents for joining large-grained commercial ceramics together at moderate temperatures because of having many short-circuit diffusion paths as a result of the high fraction of grain boundaries [7]. There are indications that nanoceramics could have extremely low thermal conductivity due to phonon scattering caused by the grain boundaries [8,9].

The formation of α-alumina occurs at temperatures as high as 1200 °C after a series of polymorphic transformations, including γ-alumina → δ-alumina → θ-alumina → α-alumina, upon heating. The α-nuclei form within the θ-alumina matrix at low temperatures and then grow rapidly to produce α-alumina colonies in the form of a porous network. The $\gamma \rightarrow \delta \rightarrow \theta$ transformations are both displacive [10,11] and have

---

*Corresponding author. Tel.: +44 1509223331; fax: +44 1509223949.
E-mail address: s.ghanizadeh@lboro.ac.uk (S. Ghanizadeh).

0272-8842/$ - see front matter © 2013 Elsevier Ltd and Techna Group S.r.l. All rights reserved.
http://dx.doi.org/10.1016/j.ceramint.2013.07.011

fairly low activation energies. However θ→α is a reconstructive transformation with high activation energy and proceeds through a nucleation and growth process [12]. Most of the activation energy for this transformation is required for the nucleation part of the process; hence temperatures up to 1200 °C are required [12]. This inevitably leads to a considerable degree of particle coarsening. The resulting, heavily aggregated, α-alumina powders then need to be mechanically milled and sintered at temperatures as high as 1600 °C in order to achieve densities near to theoretical [13,14], which results in further coarsening and grain growth. Therefore, achieving a reduction in the θ→α transformation temperature is a key requirement of forming nanostructured α-alumina powder.

Powders of α-alumina can be synthesised by several well-established synthesis methods, such as the Bayer process, sol–gel, precipitation and hydrothermal treatment [5]. However, as indicated above, with most of these methods temperatures above 1200 °C are required to produce the final crystalline α-alumina phase. The exceptions require calcinations in specific atmospheres such as hydrogen halide [15], which raises costs. A number of researchers have attempted to use seeding to increase the kinetics of the θ→α transformation and, hence, to control the development of the α-phase [13,16–19]. Kumagai and Messing [17,20] reported that by introducing α-alumina seed to boehmite gels, both the kinetics of the transformation and the microstructure of the final product could be improved. These seeded gels could be sintered to almost full density at only 1200 °C. Dynys and Halloran [12] studied the effects of introducing metal oxides such as MgO, Cr_2O_3 and Fe_2O_3 via water-soluble salts to boehmite. The results illustrated that addition of Fe_2O_3 increased the kinetics of the phase transformation to α-alumina, whereas the other oxides had no effect. Li and Sun [13] investigated the effect of the presence of ammonium nitrate (a by-product of the precipitation of aluminium nitrate and ammonia solution) and α-alumina seeding on the transformation temperature to the α-phase. It was shown that addition of 5 wt% α-alumina seeds and 44 wt% ammonium nitrate could lower the temperature of the transition from around 1200 °C to 900 °C and the final α-alumina powder had a mean particle size of ~10 nm, though it also contained the much larger seeds.

Hydrothermal synthesis is an attractive environmental friendly alternative to the approaches mentioned earlier, with the advantage of being a single-step, low energy consumption process with no need for high-temperature calcination and extensive milling [21]. Further advantages include high chemical and phase purity, low aggregation level and narrow crystallite size distribution for the resulting material, in addition to excellent control of particle morphology [1]. It is possible to produce a wide range of particle shapes, both equiaxed, such as cubes, spheres, diamonds and bipyramids, and elongated morphologies, such as fibres, whiskers, nanorods, nanotubes and also platelets, nanoribbons, nanobelts, etc. The particle size can also range from a few nanometers to large single crystals [2,22–27].

The phase relationships in the Al_2O_3–H_2O system, which were established initially by Laubengayer and Weisz [28] and subsequently studied by several other investigators such as Ervin and Osborn [29] and Kennedy [30,31], Fig. 1, revealed the presence of four phases in the temperature range of 0–500 °C and pressure range of 1–100 MPa. These phases include gibbsite $Al(OH)_3$, boehmite γ-AlOOH, diaspore α-AlOOH and α-alumina. By increasing the temperature under hydrothermal conditions, boehmite transforms either directly into the α-alumina phase at 380 °C and pressures between 1–15 MPa or into the intermediate diaspore phase from 210 °C and then into α-alumina from 360 °C at higher pressures, without forming transition aluminas. The following reactions occur under hydrothermal conditions at pressures in the range of 1–15 MPa [1]:

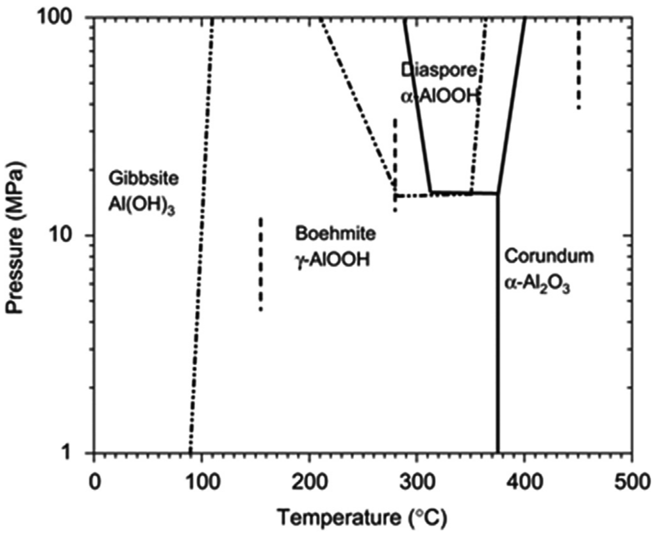

Fig. 1. Hydrothermal Al_2O_3–H_2O phase diagram from [1] with permission © 2009, The American Ceramic Society.

$$Al(OH)_3 \rightarrow \gamma\text{-}AlOOH + H_2O \text{ at } \sim 100\ ^\circ C \tag{1}$$

$$2\gamma\text{-}AlOOH \rightarrow \alpha\text{-}Al_2O_3 + H_2O \text{ at } \sim 380\ ^\circ C \tag{2}$$

A number of researchers have attempted to reduce the phase formation temperature of the α-alumina phase to < 380 °C by adding seeds to increase the kinetics of the α-alumina transformation and control the development of the desired α-phase [1,2,27]. Sharma and co-workers [2] reported the synthesis of α-alumina with a small amount of boehmite by using 4 wt% of seed with respect to the Al_2O_3 via a co-precipitation method (pH ~ 10) followed by a hydrothermal treatment under a saturated water vapour pressure at 190 °C. A mixture of two different types of surfactants was also used during the precipitation of precursors in this work in order to reduce the surface free energy of the initial particles. Characterisation showed that the synthesised α-alumina particles were about 60 nm in size with a surface area of 245 $m^2\ g^{-1}$. Hydrothermal synthesis of fine α-alumina powders using seeds in an acidic environment at 200 °C was investigated by Yang et al. [27]. The results illustrated that α-alumina powders with a maximum crystallite size of 32 nm (calculated by the Scherrer formula) could be obtained by adding 4 wt% seed relative to the amount of the starting aluminium salt.

So far, to our knowledge, most of the researches have been focused on applying seeds to different chemical routes to obtain α-alumina at lower temperatures. However, the phase transformation process to α phase in reaction-formed seeded particles has rarely been reported. The main focus of the present work was to study in detail the effects of α-alumina seeding in combination with the use of different chemical additives such as surfactants for both precipitation and hydrothermal synthesis methods with a view to controlling the size, phase and morphology of alumina nanoparticles.

2. Materials and methods

Fig. 2 shows a flow chart for the different routes used to produce the nano-alumina particles, whilst Tables 1 and 2 summarise the different experimental synthesis conditions used.

2.1. Hydrothermal synthesis

Aluminium chloride hexahydrate, $AlCl_3 \cdot 6H_2O$ (99+%, Fisher Scientific, Loughborough, UK) was used as the starting material. A precursor solution was initially prepared by dissolving the aluminium chloride in deionised water and stirring for 1 h at room temperature. Two different sets of conditions were used for the hydrothermal treatment, acidic and basic. For the former, no surfactant was needed whilst for the latter two different surfactants were investigated, viz. Tween-80 (98%, Sigma-Aldrich, Gillingham, UK) and *β*-alanine (98%, Sigma-Aldrich, Gillingham, UK). Sharma et al. used these two additives along with hydrothermal treatment to produce nanosized α-alumina [2]. In each case, 10 wt% with respect to the Al_2O_3 content was added separately to the precursor solution with further stirring for 1 h.

For both the acidic and basic routes, α-alumina powder (BMA15, Baikowski, France) with mean particle size 150 nm, as shown in Fig. 3, was gradually mixed into the solutions to act as seeds. For the acidic route 0, 1, 2, 3 and 4 wt% seeds were used whilst for the basic route just 4 wt% was added. The pH was subsequently changed; for the acidic route this involved gradually adding a 20% aqueous solution of tetraethyl ammonium hydroxide, TEAH (Merck KGaA, Darmstadt, Germany), to obtain cloudy suspensions with a pH of 3.0 ± 0.1. For the basic route, 35% ammonia solution (Fisher Scientific, Loughborough, UK) was gradually added under continuous stirring until the suspension was converted to a gelatinous precipitate with a final pH of 10.0 ± 0.1. In both cases, the precipitates were transferred into 30 ml stainless steel autoclaves lined with Teflon, filling about 70% of the autoclave volume; these were placed in an oven held at 220 °C. The pressure that developed inside the autoclave was the autogenous water vapour pressure. Subsequently, the

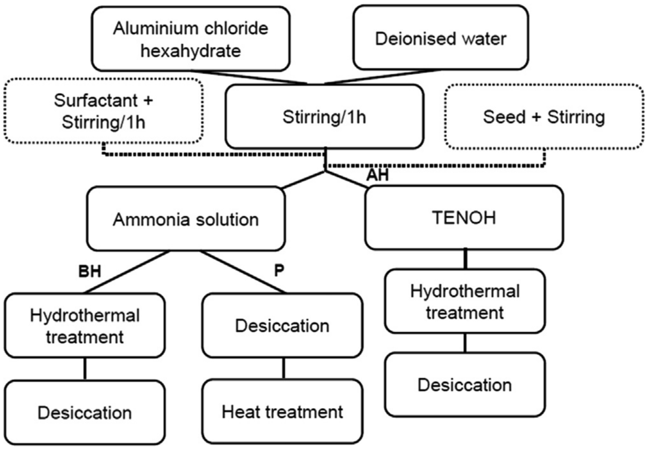

Fig. 2. Flow diagram of the different synthesis routes; AH: acidic hydrothermal, BH: basic hydrothermal, and P: precipitation.

Table 2
Summary of the precipitation synthesis conditions used for different powders.

Sample	Seed wt%	Surfactant wt%	Heat treatment
P-10-1	–	–	1000 °C/1 h
P-10-6	–	–	1000 °C/6 h
P-11-1	–	–	1100 °C/1 h
P-11-3	–	–	1100 °C/3 h
P-12-1	–	–	1200 °C/1 h
P-S4-8-6	4	–	800 °C/6 h
P-S4-8-12	4	–	800 °C/12 h
P-S8-8-12	8	–	800 °C/12 h
P-S4-10-1	4	–	1000 °C/1 h
P-S4-10-3	4	–	1000 °C/3 h
P-S4-10-6	4	–	1000 °C/6 h
P-S4-11-1	4	–	1100 °C/1 h
P-S4S10-8-12	4	10	800 °C/12 h
P-S8S10-8-12	8	10	800 °C/12 h

Table 1
Summary of the hydrothermal synthesis conditions used for different powders.

Sample	Seed wt%	Surfactant wt%	pH	Heat treatment (°C/24 h)
HA-0	–	–	∼3	220
HA-1	1	–	∼3	220
HA-2	2	–	∼3	220
HA-3	3	–	∼3	220
HA-4	4	–	∼3	220
HB-0	–	–	∼10	220
HB-4	4	–	∼10	220
HB-4-10	4	10	∼10	220

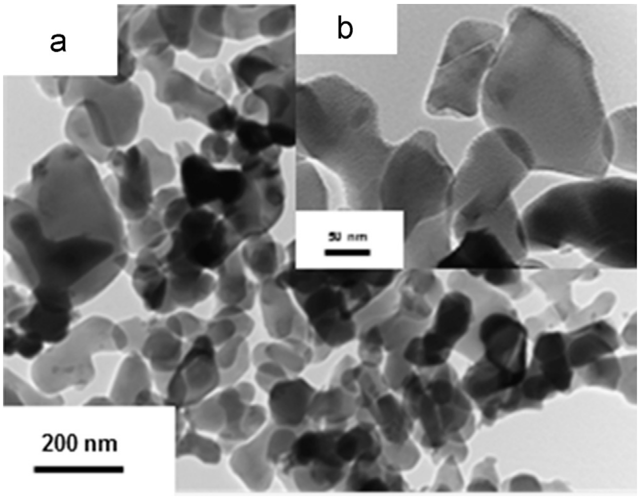

Fig. 3. TEM micrographs of the seeding powder at (a) low and (b) high magnifications.

resulting powders were washed with deionised water and absolute ethanol then separated from the liquid phase by centrifuging at 3000 rpm, desiccating in an oven at 80 °C for 24 h and ground using a pestle and mortar. As the hydroxides of alumina are soluble in acid, small amounts of each of the seeded samples were kept in 20% acetic acid solution for 30 min between washing and drying with the aim of removing any remaining aluminium hydroxide. After characterising the hydrothermally-synthesised ground powders, they were heat treated in air in a box furnace using a heating rate of 5 °C min^{-1} at 1000 °C for 6 h.

2.2. *Precipitation synthesis*

The gelatinous precipitates prepared in Section 2.1 were desiccated in an oven at 80 °C for 24 h and subsequently ground with a pestle and mortar. To study the effects of adding surfactant and seed on the phase transformations of the precursor precipitates, samples with different compositions were prepared; for the first group no α-alumina seed or surfactant was added; for the second group only α-alumina seed was introduced to the precursor gel, and for the third group a mixture of both surfactant and α-alumina seed were added, see Table 2. The ground powders were then treated in air in a box furnace using a heating rate of 5 °C min^{-1} to temperatures of 800, 1000, 1100 and 1200 °C with dwell times of 1 to 12 h.

2.3. *Powder characterisation*

The crystalline phase of the powders was determined using X-ray diffraction (Bruker D-8 Diffractometer, Karlsruhe, Germany) over the range of $2\theta = 20$–$60°$ with a scanning speed of 0.02 deg s^{-1}. The surface area and pore size distribution of the powders were measured by using an automated BET gas adsorption analyser (Tristar™ 3000, Micromeritics Instrument Corporation, Norcross, USA). The size and morphology of the particles were investigated by using transmission electron microscopy (Jeol-2000FX, Tokyo, Japan). To prepare samples for electron microscopy, an ultrasonic agitator was used to suspend the prepared powders in ethanol. After applying a small drop of the suspensions onto copper grids, they were left to dry in a sample box before being gold coated.

3. Results and discussion

3.1. *Hydrothermal synthesis*

Fig. 4 shows the XRD patterns of samples HA-0 and HA-4 (see Tables 1–3 for an explanation of the sample coding) before hydrothermal treatment, with the former sample being in an amorphous state and consisting of a broad curve without observable diffraction peaks. This indicates that amorphous aluminium hydroxide was formed by the precipitation. For sample HA-4, however, the XRD result shows the sharp peaks of the α-alumina seeds and the $Al(OH)_3$ amorphous phase. Figs. 5 and 6 show the XRD patterns for the powders produced from the acidic and basic hydrothermal routes respectively. Sample HA-0, made via the acidic route without any seeds, consisted entirely of boehmite, whilst samples HA-1 to HA-4 show decreasing amounts of boehmite compared to α-alumina as the amount of seeds added increased. Although the seeded post-hydrothermal powders were washed in acetic acid solution, traces of boehmite identified in all the samples proved that aluminium oxyhydroxide could not be entirely washed away. For sample HA-4, which contained 4 wt% seeds, the only phase detected was α-alumina.

For the powders synthesised via the basic route, Fig. 6, before the hydrothermal treatment at 220 °C for 24 h, sample HB-0 (Fig. 6a) showed sharp peaks of crystalline ammonium chloride (salammoniac). However some weak broad peaks, highlighted by the arrows, were observed as well; these coincided with those of boehmite (AlOOH, aluminium oxyhydroxide, JCPDS 88-2112). This showed that the

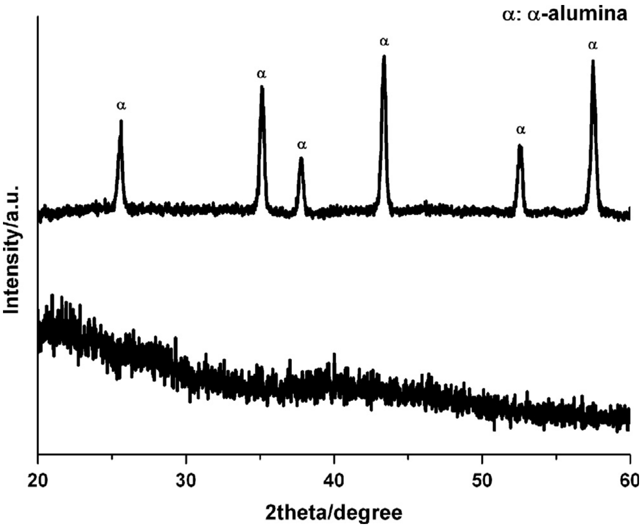

Fig. 4. XRD patterns of samples (a) HA-0 and (b) HA-4 before hydrothermal treatment.

Table 3
Phases present after calcinations in the powders synthesised by precipitation.

Sample	Phases detected by XRD
P-10-1	θ
P-10-6	α+∼50% θ
P-11-1	α+traces of θ
P-11-3	α
P-12-1	α
P-S4-8-6	θ
P-S4-8-12	α+∼50% θ
P-S8-8-12	α+∼45% θ
P-S4-10-1	α+∼20% θ
P-S4-10-3	α+∼10% θ
P-S4-10-6	α
P-S4-11-1	α
P-S4S10-8-12	α+∼40% θ
P-S8S10-8-12	α+∼35% θ

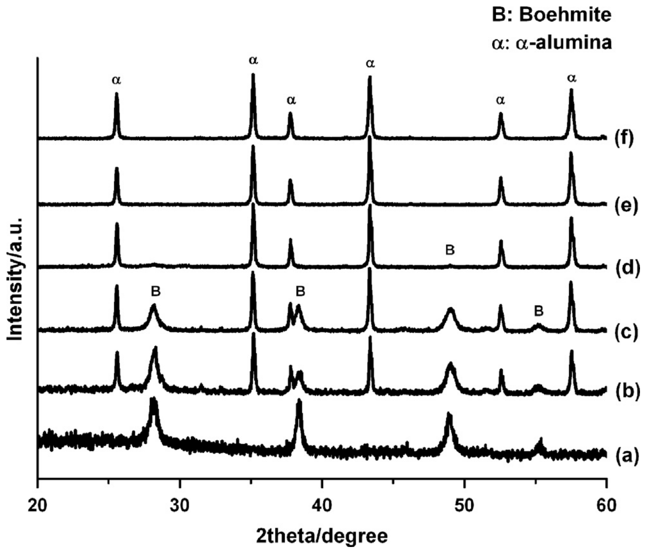

Fig. 5. XRD patterns of samples (a) HA-0, (b) HA-1, (c) HA-2, (d) HA-3 and (e) HA-4 after hydrothermal treatment at 220 °C for 24 h and (f) HA-4 after being heat treated at 1000 °C.

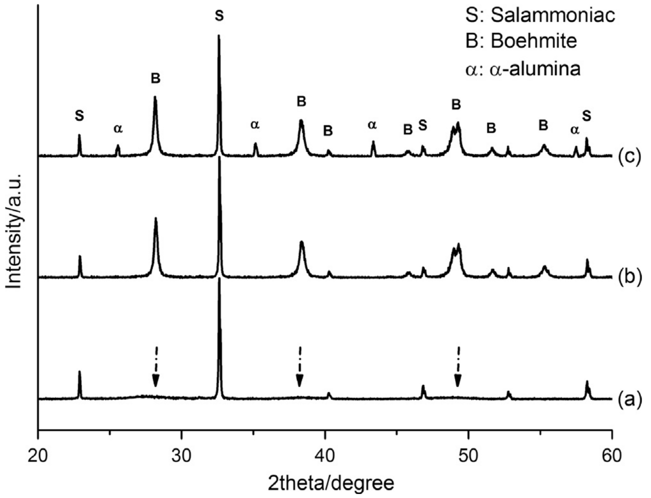

Fig. 6. XRD patterns of sample HB-0 (a) before and (b) after hydrothermal treatment at 220 °C for 24 h and sample HB-4 (c) after the same hydrothermal treatment and (d) after being heat treated at 1000 °C.

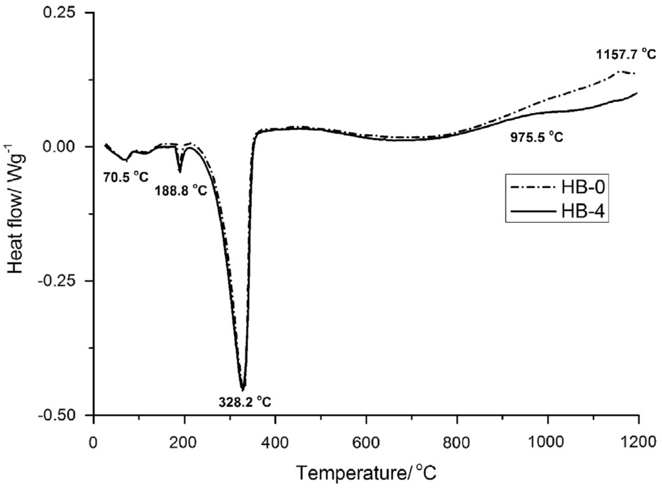

Fig. 7. Thermal analysis of hydrothermally-prepared samples HB-0 and HB-4.

pseudoboehmite phase was formed during the precipitation process; the formation of this phase at high pH was due to the excess amount of hydroxyl groups coming from NH_4OH. After the hydrothermal treatment, as shown in (Fig. 6b), the fraction of the boehmite phase increased substantially. When α-alumina seeds were added, HB-4 (Fig. 6c), small amounts of α-alumina were observed along with the boehmite and salammoniac. Note that washing the post-hydrothermal powders with deionised water and absolute ethanol did not help to remove the ammonium chloride phase present in the samples and the 30 min wash in acetic acid solution did not succeed in removing the boehmite, though the XRD peaks indexed as boehmite did disappear after the powder was heat treated at 1000 °C, as demonstrated in (Fig. 6d).

Upon heating, the boehmite phase goes through a series of polymorphic transformations including $\gamma \rightarrow \delta \rightarrow \theta \rightarrow \alpha$ before reaching the stable α-alumina form [13]. Thermal analysis of samples HB-0 and HB-4, Fig. 7, showed two endothermic peaks existing at 70.5 °C and 188.8 °C for both samples. The former was due to the evaporation of absorbed water and the latter was caused by removal of the structural water existing in the oxyhydroxide phase. There was a noticeable endothermic peak at 328.5 °C for both samples, which was compatible with the decomposition point of ammonium chloride and was associated with sublimation of this material present in the samples as the by-product of the synthesis process. There was an exothermic peak at 975.5 °C and 1157.7 °C for HB-0 and HB-4 samples, respectively, which was caused by θ-alumina → α-alumina phase transformation.

Transmission electron micrographs of the powders synthesised via the acidic and basic routes are shown in Figs. 8 and 9 respectively. For sample H-A-0, Fig. 8a, only the typical acicular (needle-like) boehmite particles were observed, whilst as the amount of α-alumina seeds increased the fraction of α-alumina particles in the TEM micrographs also increased, as shown in Fig. 8b and c. However, although for sample HA-4

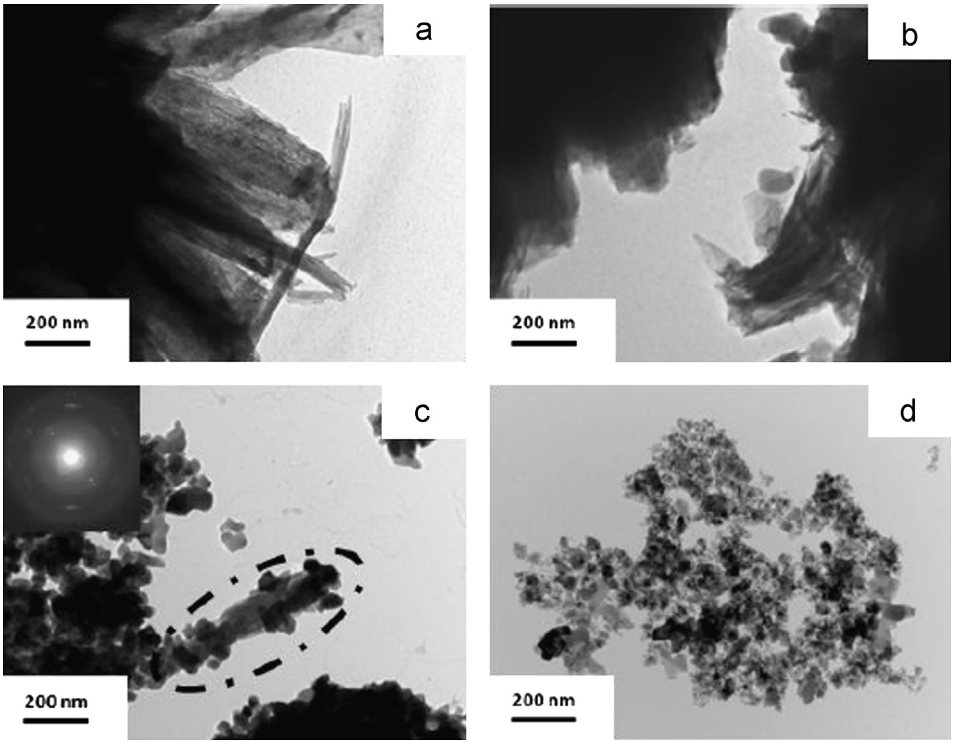

Fig. 8. TEM micrographs of powders after hydrothermal treatment at 220 °C for 24 h (a) HA-0, (b) HA-1 and (c) HA-4, inset top left the SAEP of the highlighted acicular particles and (d) shows sample HA-4–10 after heat treatment at 1000 °C.

no diffraction peak related to boehmite was observed in the XRD results, the TEM investigation showed the presence of acicular particles in this sample, the SAEP of which is presented in Fig. 8c top left inset. This is consistent with the presence of boehmite. The latter structure transformed to fine α-alumina particles after being heat treated at 1000 °C, Fig. 8d, where the large particles in the micrograph represent the seeds and the finer ones are the synthesised α-alumina particles. The images in Fig. 9 are very similar. The non-seeded sample, HB-0, displays typical acicular boemite particles, as shown in Fig. 9a, whilst the addition of seeds led to the formation of a bimodal morphology consisting of the acicular particles and their agglomerates and more equiaxed α-alumina particles, Fig. 9b and c. After heat treatment at 1000 °C the boehmite particles transformed to fine α-alumina particles, Fig. 9d, similar to what was observed via the acidic route.

Comparison of the above results revealed that when similar conditions of hydrothermal treatment and 4 wt% seed addition were used, the acidic route led to the pure α-alumina phase, at least to the limit of resolution of X-ray diffraction, whilst the basic route led to a powder that still retained significant quantities of boehmite and ammonium salts. However, the amounts of powder produced by the acidic route were considerably less than the powder made by the basic route. This might be because the basic aluminium salts are highly soluble and can be precipitated only at a high OH/Al ratio [32]. Therefore, during the acidic route at pH∼3 less precipitate was formed compared to the basic route. This resulted in less amount of boehmite after the hydrothermal treatment, which could not be fully detected in the samples, particularly those with 4 wt%-seeds due to the limited resolution of X-ray diffraction and the high fraction of α-alumina seed used. This assumption, along with the fact that the morphology of the α-alumina particles in the final powder was very similar to the seeding powder, suggests that the low amount of α phase detected after the hydrothermal treatment could be primarily the α-alumina seeds added to the precursor solution during the initial precipitation process.

3.2. Precipitation synthesis

The phases detected by XRD are presented in Table 3 for each of the powders formed. It can be seen that higher temperatures and/or longer times led to a greater fraction of α-alumina in the final powder, as expected; similar results have been reported by other researchers [13,20]. When α-alumina seeds were added, the conditions required to form the α-alumina phase were significantly reduced. For example, for unseeded samples either 3 h at 1100 °C or 1 h at 1200 °C were required to produce powder in which no θ phase could be detected by XRD. When 4 wt% of seeds were included, either 1 h at 1100 °C or 6 h at 1000 °C was sufficient to avoid the theta phase. A temperature as low as 800 °C, albeit for 12 h, could be used to achieve an approximately 50/50 mix of α and θ-alumina when the seeds were used; without the seeds 1000 °C for 6 h was required to achieve a similar result. This reduction in the formation temperature of α-alumina is due to the effect of seeding, which can be described by the heterogeneous nucleation theory. As each of the added seeds provided multiple nucleation sites for phase transformation to

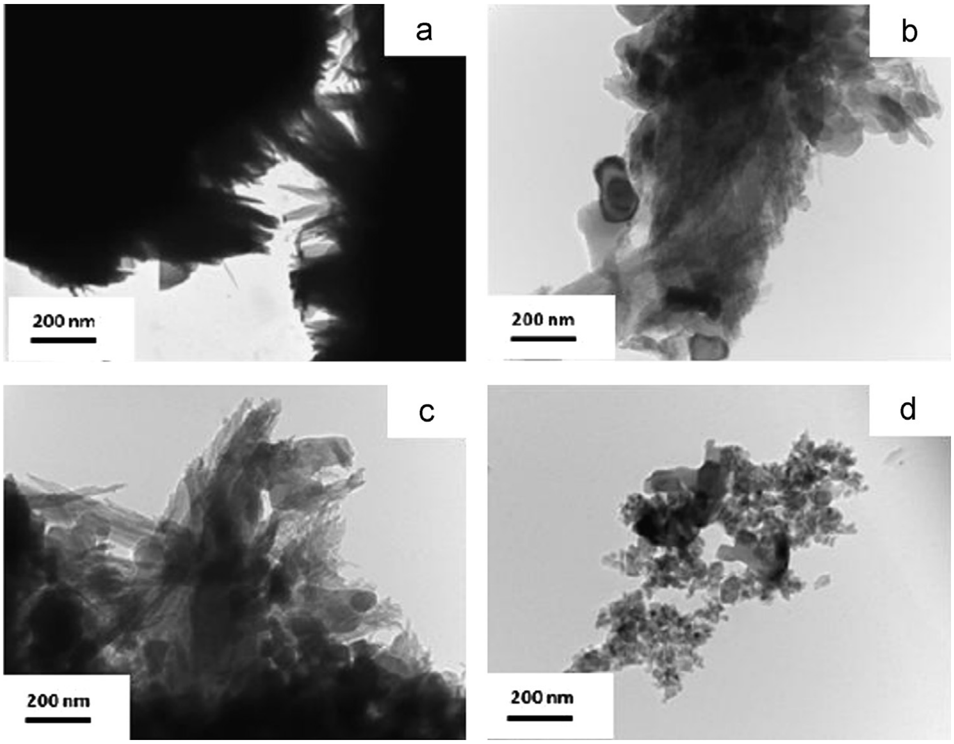

Fig. 9. TEM micrographs of powders (a) HB-0, (b) HB-4 and (c) HB-4-10 after hydrothermal treatment at 220 °C for 24 h, (d) shows sample HB-4-10 after heat treatment at 1000 °C.

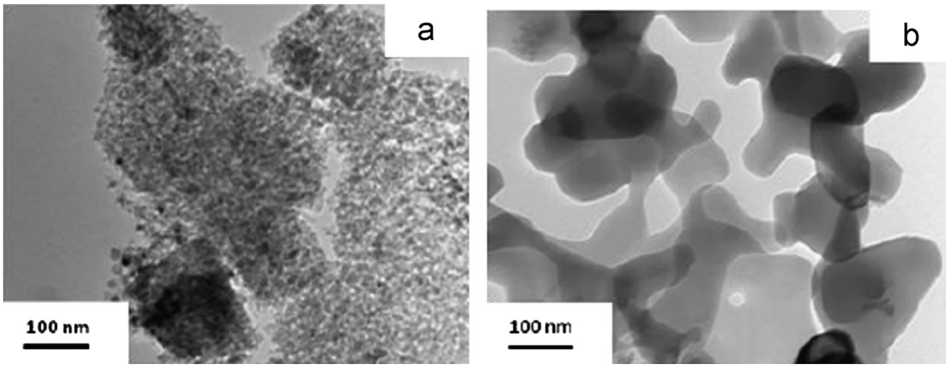

Fig. 10. TEM micrographs of unseeded powders after calcination (a) P-10-6 and (b) P-12-1.

α-alumina, the transformation kinetics increased considerably and as a result the transformation temperature was lowered [13,33,34].

TEM investigation of the non-seeded samples revealed that calcination at 1000 °C for 1 h yielded ~20 nm particles of θ-alumina, Fig. 10a. The surface area of this powder measured by the BET method was 122.4 $m^2\,g^{-1}$, leading to a calculated average particle size of 12 nm, which was approximately compatible with the TEM results.

To obtain only α-alumina particles required calcination at temperatures as high as 1200 °C, although these conditions yielded particles with a mean size of about 200 nm, Fig. 10b. The average particle size of this powder was calculated to be 185 nm using the BET surface area value of 8.1 $m^2\,g^{-1}$. The pore size distribution trends of powders P-10-6 and P-12-1 are demonstrated in Fig. 11. In comparison to the monomodal pore

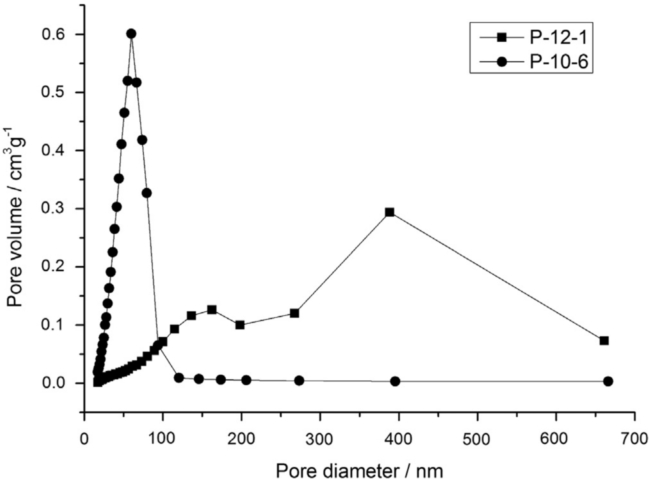

Fig. 11. Pore size distribution of powders P-10-6 and P-12-1.

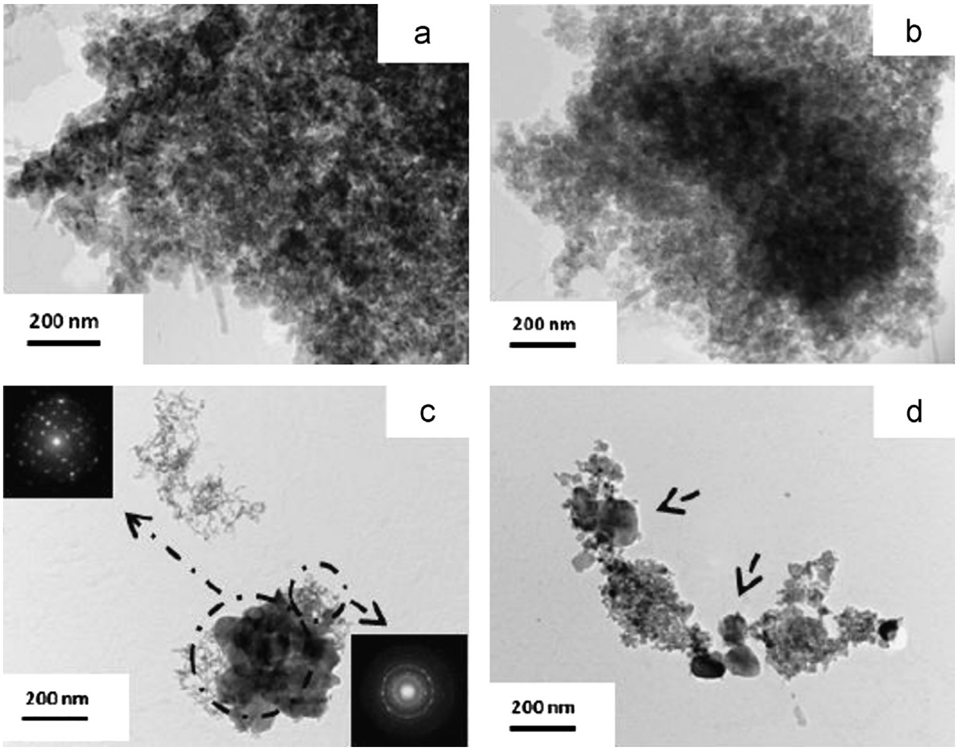

Fig. 12. TEM micrographs of samples (a) P-S4-8-12 and (b) P-S8-8-12 and after adding dispersant samples (c) P-S4S10-8-12, inset top left the SAEP of highlighted large particles and bottom right the SAEP of highlighted ultra-fine particles and (d) P-S8S10-8-12, seed particles are highlighted with arrows.

size distribution of the former, the bimodal nature of P-12-1 suggested that the powder was agglomerated due to the high temperature heat treatment. The peak at ~170 nm is probably the intra-agglomerate porosity, whilst that at ~400 nm can be corresponded to the inter-agglomerate pores. When seeds were added to the precursor solution, the results were highly agglomerated ultra-fine particles of θ and α-alumina along with the seed particles, Fig. 12a and b, matching the results from the XRD.

The introduction of surfactant to the initial precursor solution had negligible effect on the amount of α-alumina phase observed in the calcined powder. As shown by the XRD results displayed in Table 3, samples P-S4S10-8-12 and P-S8S10-8-12 each contained approximately 10% less θ-alumina, and hence 10% more α-alumina, than P-S4-8-12 and P-S8-8-12 respectively, the equivalent samples without surfactant. The TEM micrograph of the former is displayed in Fig. 12c, where the top left inset presents the SAEP of the agglomerated areas showing ring patterns consistent with those of both θ and α-alumina and the bottom right inset showing sharp diffraction spots corresponding to α-alumina, which could be due to the presence of the alumina seeds. As can be observed in Fig. 12c and d, where the addition of surfactant did help was in reducing the degree of agglomeration of the gelatinous precipitate and also the seeding powder, due to the surfactant interaction with the particle surface in order to reduce the particle surface free energy, which resulted in softer and less-agglomerated powder with higher fraction of α-alumina after heat treatment. Powders P-S4-8-12 and P-S4S10-8-12 possessed BET surface area values of 32.5 and 34.6 $m^2\ g^{-1}$, respectively. The slightly higher surface area value of the latter could be due to the presence of surfactant in the initial solution prior to precipitation, which led to a lower level of agglomeration in the final powder.

4. Conclusions

The addition of α-alumina seeds during the low temperature hydrothermal treatment (≤220 °C), as a direct transformation route without the formation of transient alumina, was not successful in obtaining α-alumina powder in both basic and acidic atmospheres under a saturated water vapour pressure Crystalline boehmite was the only phase formed in both hydrothermally-synthesised non-seeded and seeded samples along with traces of α-alumina due to the existence of seed crystals. In order to obtain α-alumina powder via the hydrothermal method at low pressures, higher temperatures, ≥380 °C, need to be investigated.

The precipitation method was also used to synthesise fine α-alumina powders from aluminium chloride and ammonia solution. It was shown that by seeding the initial precipitate, the temperature of the $\theta\text{-Al}_2\text{O}_3 \rightarrow \alpha\text{-Al}_2\text{O}_3$ transformation could be lowered to 800 °C. The presence of sufficient amount of seeds have been reported to lower the θ→α transformation temperature, as seeding decreases the activation energy of the nucleation process [13,17–19].

Introducing 10 wt% of a mixture of two surfactants to the precipitate, led to less agglomeration and higher fraction of α phase present in the powders heat treated at temperatures as low as 800 °C by modifying both the surface of the primary particles and also the seed particles added to the precipitate.

References

[1] W.L. Suchanek, Hydrothermal synthesis of alpha alumina (α-Al_2O_3) powders: study of the processing variables and growth mechanisms, Journal of the American Ceramic Society 93 (2010) 399–412.

[2] P.K. Sharma, M.H. Jilavi, D. Burgard, R. Nass, H. Schmidt, Hydrothermal synthesis of nanosize α-Al_2O_3 from seeded aluminum hydroxide, Journal of the American Ceramic Society 81 (1998) 2732–2734.

[3] E. Straßburger, Ballistic testing of transparent armour ceramics, Journal of the European Ceramic Society 29 (2009) 267–273.

[4] A. Krell, J. Klimke, T. Hutzler, Advanced spinel and sub-μm Al_2O_3 for transparent armour applications, Journal of the European Ceramic Society 29 (2009) 275–281.

[5] C.P. Poole, F.J. Owens, Introduction to Nanotechnology, 1st ed., Wiley-Interscience, New Jersey, 2003.

[6] M. Wilson, Nanotechnology: Basic Science and Emerging Technologies, 1st ed., CRC Press, Sydney, 2002.

[7] T.H. Cross, M.J. Mayo, Ceramic-ceramic diffusion bonding using nanocrystalline interlayers, Nanostructured Materials 3 (1993) 163–168.

[8] R.W. Kelsall, I.W. Hamley, M. Geoghegan, J. Wiley, Nanoscale Science and Technology, 1st ed., Wiley Online Library, Chichester, 2005.

[9] F.R. Charvat, W.D. Kingery, Thermal conductivity: XIII, effect of microstructure on conductivity of single-phase ceramic, Journal of the American Ceramic Society 40 (1957) 306–315.

[10] B.C. Lippens, J.H. De Boer, Study of phase transformations during calcination of aluminum hydroxides by selected area electron diffraction, Acta Crystallography 17 (1964) 1312–1321.

[11] S.J. Wilson, The dehydration of boehmite, γ-AlOOH, to γ-Al_2O_3, Journal of Solid State Chemistry 30 (1979) 247–255.

[12] F.W. Dynys, J.W. Halloran, Alpha alumina formation in alum-derived gamma alumina, Journal of the American Ceramic Society 65 (1982) 442–448.

[13] J.G. Li, X. Sun, Synthesis and sintering behavior of a nanocrystalline α-alumina powder, Acta Materialia 48 (2000) 3103–3112.

[14] P.K. Sharma, V.V. Varadan, V.K. Varadan, A critical role of pH in the colloidal synthesis and phase transformation of nano size α-Al_2O_3 with high surface area, Journal of the European Ceramic Society 23 (2003) 659–666.

[15] M. Mohri, Y. Uchida, Y. Sawabe, H. Watanabe, Inventors, Anonymous α-Alumina Powder and Process for Producing the Same, US Patent 6159441, 2000.

[16] M. Kumagai, G.L. Messing, Enhanced densification of boehmite sol–gels by α-alumina seeding, Journal of the American Ceramic Society 67 (1984) c230–c231.

[17] M. Kumagai, G.L. Messing, Controlled transformation and sintering of a boehmite sol–gel by α-alumina seeding, Journal of the American Ceramic Society 68 (1985) 500–505.

[18] L. Pach, R. Roy, S. Komarneni, Nucleation of alpha alumina in boehmite gel, Journal of Materials Research 5 (1990) 278–285.

[19] S. Rajendran, Production of ultrafine alpha alumina powders and fabrication of fine grained strong ceramics, Journal of Materials Science 29 (1994) 5664–5672.

[20] G.L. Messing, M. KumagaI, Low-temperature sintering of alpha-alumina-seeded boehmite gels, American Ceramic Scoiety Bulletin 73 (10) (1994) 88–91.

[21] K. Byrappa, M. Yoshimura, Handbook of Hydrothermal Technology: a Technology for Crystal Growth and Materials Processing, 1st ed, William Andrew, New York, 2001.

[22] W.L. Suchanek, M.M. Lencka, R.E. Riman, Hydrothermal synthesis of ceramic materials, in: D.A. Palmer, R. Fernandez-Prini, A.H. Harvey (Eds.), Aqueous Systems at Elevated Temperatures and Pressures: Physical Chemistry in Water, Steam and Hydrothermal Solutions, Elsevier, Amsterdam, 2004, pp. 717–744.

[23] R.E. Riman, W.L. Suchanek, M.M. Lencka (Eds.), Annales de Chimie Science des Matériaux, Elsevier, Paris, 2002.

[24] K. Byrappa, T. Adschiri, Hydrothermal technology for nanotechnology, Progress in Crystal Growth and Characterization of Materials 53 (2007) 117–166.

[25] J.H. Adair, E. Suvaci, Morphological control of particles, Current Opinion in Colloid and Interface Science 5 (2000) 160–167.

[26] M. Yoshimura, K. Byrappa, Hydrothermal processing of materials: past, present and future, Journal of Materials Science 43 (2008) 2085–2103.

[27] J. Yang, S. Mei, J.M.F. Ferreira, Hydrothermal synthesis of submicrometer α-alumina from seeded tetraethylammonium hydroxide-peptized aluminum hydroxide, Journal of the American Ceramic Society 86 (2003) 2055–2058.

[28] A.W. Laubengayer, R.S. Weisz, A hydrothermal study of equilibria in the system alumina–water, Journal of the American Ceramic Society 65 (1943) 247–250.

[29] E. Ervin, E. Osborn, The system Al_2O_3–H_2O, Journal of Geology 59 (1951) 381–394.

[30] G.C. Kennedy, Phase relations in the system of Al_2O_3–H_2O at high temperatures and pressures, American Journal of Science 257 (1959) 563–573.

[31] E.M. Levin, C.R. Robbins, H.F. McMurdie, Phase Diagrams for Ceramists, 1st ed., American Ceramic Society, Ohio, 1964.

[32] F. Xiao, B. Zhang, C. Lee, Effects of low temperature on aluminum (III) hydrolysis: theoretical and experimental studies, Journal of Environmental Sciences 20 (2008) 907–914.

[33] J. McArdle, G. Messing, Transformation and microstructure control in boehmite-derived alumina by ferric oxide seeding, Advanced Ceramic Materials 3 (1988) 387–394.

[34] R. Shelleman, G. Messing, M. Kumagai, Alpha alumina transformation in seeded boehmite gels, Journal of Non-crystalline Solids 82 (1986) 277–285.